Title

Intrinsic apoptosis is evolutionarily divergent among metazoans

Authors

Gabriel Krasovec [1,2*], Éric Quéinnec [1**], Jean-Philippe Chambon [3**]

[*] Authors for correspondence:

GK, gabriel.krasovec@universityofgalway.ie; gabrielkrasovec@hotmail.fr

[**] These authors share senior authorship.

Affiliations

[1]ISYEB, Institut de Systématique, Evolution et Biodiversité, Sorbonne Université, CNRS, MNHN, F-75252 Paris Cedex 05, France.

[2]Centre for Chromosome Biology, School of Natural Sciences, National University of Ireland Galway, Galway, Ireland.

[3]CRBM, Univ. Montpellier, CNRS, 34000 Montpellier, France

Abstract

Apoptosis is regulated cell death that depends on caspases. Upstream of each apoptotic signalling pathway is involved a specific initiator caspase. Characterised in nematode, fly and mammals, intrinsic apoptosis is considered to be ancestral and conserved among animals, and depends on shared initiators; caspase-9*,* Apaf-1 and Bcl-2. However, the biochemical role of mitochondria, the pivotal function of cytochrome c and the modality of caspase activation remain highly heterogeneous and hide profound molecular divergences among apoptotic pathways in animals. Uncovering the phylogenetic history of apoptotic actors, especially caspases, is crucial to shed light on intrinsic apoptosis evolutionary history. Here, we demonstrate by phylogenetic analyses, that caspase-9, the fundamental key of intrinsic apoptosis, is deuterostome-specific, while caspase-2 is ancestral to bilaterians. Our analysis of Bcl-2 and Apaf-1 confirm heterogeneity in functional organisation of apoptotic pathways in animals. Our results support emergence of distinct intrinsic apoptotic pathways during metazoan evolution.

44 **INTRODUCTION**

45 Apoptosis, regulated cell death defined by a set of morphological features and
46 dependent on caspases, occurs during metazoan development, tissue homeostasis, and
47 regeneration[1–3]. Pioneering works in *Caenorhabditis elegans* established a molecular network
48 of apoptosis decision, execution, engulfment-degradation, and more fundamentally the first
49 description of intrinsic apoptosis, previously known as the mitochondrial apoptotic pathway[4–
50 6]. Next, investigation of apoptotic cascade key components from *Drosophila melanogaster* and
51 mammals imposed the paradigm that the intrinsic apoptotic "molecular program" is
52 conserved throughout animal evolution[4,5,7–9]. Intrinsic apoptosis depends on the key initiator
53 caspase-9 (named Ced-3 and Dronc in *Caenorhabditis* and *Drosophila*, respectively), the
54 activator Apaf-1 (named Ced-4 and Dark in *Caenorhabditis* and *Drosophila*, respectively) and
55 the Bcl-2 multigenic family[4,8]. However, recent research has revealed evolutionary
56 divergences between these models, with major functional diversifications[10,11]. Importantly
57 and independently of functional approaches, the phylogenetic history of the signal
58 transduction actors, mostly the caspase family, is the Rosetta Stone to shed light on intrinsic
59 apoptosis evolution. Here, we investigate the evolutionary genetic history of the major actors
60 of intrinsic apoptosis. We conducted phylogenetic analyses of initiator CARD-caspases, Bcl-2
61 multigenic family, and Apaf-1 proteins from major animal phyla and describe their
62 evolutionary patterns. Despite common functional similarities, these actors, especially
63 initiator caspases, are engaged in relatively independent evolutionary histories that involve
64 different signalling pathways. Consequently, we consider the structural similarities of intrinsic
65 apoptotic components to be the result of convergent evolution among animals. Convergent
66 evolution is defined here as a set of patterns (i.e. named intrinsic apoptosis) produced by
67 similar but not identical processes (i.e. pathways driven by at least two groups of paralogous

genes). Thus, the classical animal models (nematode, fly, mouse) which were used to establish a unified concept of intrinsic apoptosis are markedly distinguished by distinct molecular origin of their apoptotic actors but also by major functional divergences.

RESULTS AND DISCUSSION

Initiator caspases of intrinsic apoptotic pathways are not homologous genes

Initiation and execution of apoptotic signalling pathways are fundamentally linked to the complex diversification of caspases which are widely distributed among all metazoan phyla[12–15].

Caspases are a class of proteases composed of three protein domains; the pro-domain, the small P10, and the large P20[16,17]. Initiator caspases, specific to each apoptotic pathway, have a Caspase Recruiting Domain (CARD) pro-domain or two Death Effector Domains (DED) pro-domains. Intrinsic and extrinsic apoptosis are distinct and involve specific initiators which are caspase-9 (CARD pro-domain) or caspase-8 or -10 (DED pro-domains), respectively. Both pathways trigger activation of common executioner caspases, leading to apoptosis execution[4,18].

Due to the pivotal role of caspase-9 in initiating intrinsic apoptosis, our main analyses focused on caspases having a CARD pro-domain (CARD-caspases). We confirmed their distribution in most animal phyla and reconstructed their phylogenetic relationships (Figure 1, Table S1). Regardless of the phylogenetic methodology used for the analysis, two strongly supported (PP> 0.99) monophyletic groups were identified: caspase-9 and caspase-2 (Figure 1, Figure S1). A third and more heterogeneous group named here [Inflammatory Caspases + Caspase-Y] is monophyletic in Bayesian analysis, the method which produced the most likely topology (Table S2), and splits into two groups in maximum likelihood estimation (Figure 1,

92 Figure S1). Although relationships among bilaterian clades differ depending on the
93 methodology employed, monophyly of caspase-9 and caspase-2 families remains robust. They
94 group together with Inflammatory Caspases and Caspase-Y in a clade strictly diversified within
95 bilaterian animals (PP = 0.87; BS>90). The sequences of non-bilaterians [Cnidaria + Ctenophora
96 + Placozoa] form a divergent paraphyletic group named here Caspase-X (Figure 1). Switching
97 between metazoan putative "basal" out groups [i.e. *Amphimedon queenslandica* (Porifera) or
98 *Pleurobrachia bachei* (Ctenophora)] does not affect caspase topology (Figure S2). All
99 bilaterians sequences, caspase-9, caspase-2 and [Inflammatory Caspases + Caspase-Y] remain
100 monophyletic (Figure S2).

101 Caspase-2 appears to be widely distributed among bilaterians and sequences evolution
102 is congruent with the bilaterian groups [Deuterostomia + Ecdysozoa +
103 Lophotrochozoa/Spiralia] reflecting its ancestral origin. Surprisingly caspase-9 is strictly
104 restricted to deuterostome animals. This distribution can be interpreted either as the early
105 emergence of caspase-9 in all bilaterians followed by a secondary loss in protostomes, or as a
106 specific derived character of deuterostomes. The diversity of the genomes explored, and their
107 depth of sequencing unambiguously confirms this result. More specifically, the robustness of
108 the deuterostome caspase-9 clade was explored (Figure S3), and its specific diversification
109 among [Vertebrata + Cephalochordata + Echinodermata + Hemichordata] was confirmed.
110 However, the relative position of the cephalochordate *Branchiostoma belcheri* 9A paralogous
111 gene remains unstable. Consistent with previous studies on the ascidian *Ciona intestinalis*[19],
112 the five representatives of ascidian genomes studied are devoid of any caspase-9, likely due
113 to a unique secondary loss in urochordates, the sister-group of vertebrates[20].

114 Unexpectedly, *Drosophila* Dronc and *Caenorhabditis* Ced-3 are distinctly identified as
115 orthologous (i.e. coming from speciation) to caspase-2 of vertebrates, and not to caspase-9,

116 as was previously reported and largely accepted[21–28]. All Dronc/Ced3 proteins of insects,
117 horseshoe crab (Xiphosura), and nematodes form a strongly supported monophyletic clade
118 (PP = 1) revealing single gene conservation without duplication (except horseshoe crab). Thus,
119 the caspase-2 clade of ecdysozoans is the sister group of caspase-2 clade of [Lophotrochozoa
120 + Deuterostomia]. The absence of identifiable caspase-2 in echinoderms and hemichordates
121 (i.e. Ambulacraria) can probably be interpreted as a clade-specific derived loss.

122 Conversely, the clade [Caspase-Y + Inflammatory Caspase] appears to be restricted to
123 [Vertebrata and Lophotrochozoa].

124 To test evolutionary history and shuffling of different domains, we inferred
125 recombination rate from CARD-Caspase coding sequences (reflecting intra-codon
126 recombination). We investigated multiple alignments of domains sequences using the
127 approximate Bayesian computation (ABC) approach based on coalescent evolutionary history
128 of protein sequences, i.e. the framework *ProteinEvolverABC*[29]. The remarkable low level of
129 recombination rate (Rho mean = 2.0328712) we estimated during CARD-Caspase family
130 evolution rule out potential phylogenetic reconstruction artefacts (Table S3). As illustrative
131 examples, this low recombination rate is comparable to those observed for some
132 Coronaviruses protein families such as NS12.7 or astroviruses viroporins probably related to
133 the maintenance of viral pathogenicity[29–31]. The multiple and essential roles played by the
134 CARD-Caspase family within the cell is likely one factor explaining the extremely low
135 recombination rate that can be observed.

136 Taken globally, our analysis shows that the traditionally considered conserved initiator
137 caspases of intrinsic apoptosis are not orthologous, but are divergent genes putatively issued
138 from ancestral duplication (i.e. paralogous genes) among bilaterians.

139

140 **The caspase activation regulator apoptosome is structurally divergent in metazoans**

141 In intrinsic apoptosis, initiator caspase activation depends on their recruitment by a
142 pivotal, and considered shared component, the apoptosome platform[4,10]. Apoptosome
143 formation results on critical protein binding between *Caenorhabditis* Ced-4, *Drosophila* Dark,
144 and human Apaf-1 with their respective initiator caspases Ced-3, Dronc, and procaspase-9,
145 respectively[10]. CARD and other domains (NOD, arm) are highly conserved in Apaf-1, Dark and
146 Ced-4 proteins[32–34]. However, excepted the majority of nematode species[11], Apaf-1 possesses
147 WD40 repeats at its C-terminus which bind to cytochrome c. This binding is required in
148 mammals for Apaf-1 oligomerisation and apoptosome formation[34,35], while Ced-4 and Dark do
149 not require cytochrome c for their general assembly into an apoptosome[10,36]. Taken with
150 major structural and regulating assembly differences between the octameric Dark, tetrameric
151 Ced-4 and heptameric Apaf-1 apoptosomes, it reveals evolutionary divergence between
152 animal apoptosomes formation and procaspases activation mechanisms, probably
153 differentially modulating the cell death execution pathway[37].

154 We conducted exhaustive studies by reciprocal BLAST and phylogenetic analyses of
155 Apaf-1 homologs and confirmed their conservation in the majority of metazoan phyla (Figure
156 S4, Table S4)[32,33]. We conducted our analysis with all sequences issued from a previous study[33]
157 supplemented with ones we have specifically identified. However, we have differentiated in
158 our study Apaf-1 genes sharing a CARD domain, and likely involved in apoptosis regulation,
159 from Apaf-1-like devoid of CARD domains but which possess a panel of unusual domains. NB-
160 ARC being the most conserved and shared domain by almost all Apaf-1 and Apaf-1-like genes
161 among metazoans, we conducted the analysis on the NB-ARC alignment as it was previously
162 done[33].

163 Our topology presents two main clades that are common between Bayesian inference
164 method and maximum likelihood estimation, both of which are inconsistent with species
165 phylogeny. One of them grouped ecdysozoan sequences including Ced-4 and Dark in addition
166 to several Apaf-1-like from the cnidarian *Nematostella vectensis* and the cephalochordate
167 *Branchiostoma floridae*, while the other one contains deuterostomian and non-bilaterian
168 sequences. Unexpectedly, deuterostomians are not monophyletic but split into two groups,
169 suggesting classic Long Branch attraction artifact and a very fast sequence evolution.
170 Remarkably, Apaf-1 was absent from all available urochordate and mollusc genomes, in
171 accordance with previous work[19,33,38–41], and from *Capitella teleta* (Annelida). Even if
172 differences in the quality of the genomes might account for some of the putative losses, these
173 results suggest independent losses in urochordates and lophotrochozoans or, a less
174 parsimonious hypothesis, complex and independent modular protein evolution from the
175 common ancestor of metazoans (Figure 2). In non-bilaterians, the Apaf-1 gene family has not
176 been found in the *Pleurobrachia pileus* genome (Ctenophora), but seems present in other
177 early diverging metazoan phyla [Porifera, Cnidaria and Placozoa] ([33,42,43], our data).
178 Importantly, a previous analysis from several genomes (cnidarian, nematode, fly,
179 amphioxus, sea urchin, human) clearly identified three well-defined independent clades of
180 genes among metazoans, highlighting that Ced-4, Dark and Apaf-1 are not homologous genes
181 between ecdysozoans and vertebrates[33].
182 Despite its fundamental role in the apoptotic cell death pathways and also in non-
183 apoptotic functions[44–46], diverse metazoan phyla have independently experienced adapter
184 protein Apaf-1 losses. Apaf-1 with CARD-domain, likely involve in apoptosis, are under strong
185 purifying selection as illustrated by the metric non-synonymous/synonymous substitution rate
186 ratio (dN/dS) close to 0 (model M0; $\omega\theta = 0.07$), perhaps promoted by their crucial and specific

187 role as caspase activator. Consequently, we hypothesise a relaxation of functional constrains
188 on unusual Apaf-1 molecules (i.e. deprived of Card-domain, and probably not involved in
189 oligomerisation processes) that specifically drive the diversification of Apaf-1/Apaf-1-like
190 paralogous genes in the cnidarian *Nematostella vectensis* and the cephalochordate
191 *Branchiostoma floridae*[33].

192 These elements argue in favour of distinct evolutionary trajectory between species and
193 convergence of the modality of apoptosome formation, which could explain functional
194 analyses showing that its formation and the subsequent caspase activation differs among
195 taxa[11].

196

197 **The regulation of apoptosis by the Bcl-2 family is divergent among metazoans**

198 Intrinsic apoptosis is ultimately regulated by the Bcl-2 proteins, composed of several
199 Bcl-2 homologous (BH) domains[47,48]. In mammals, the balance between pro-survival (four
200 BH1-BH4 domains) and pro-apoptotic proteins (Bax/Bak/Bok and BH3-only) of Bcl-2 controls
201 initiation of intrinsic apoptosis. Conformational changes of the three-dimensional structures
202 and interactions between Bcl-2 actors enables the assembly of pore-like structures controlling
203 MOMP[49].

204 Multiple sequence alignments of metazoan Bcl-2 family proteins (Figure S5, Table S5)
205 (but with over-represented chordates reflective of greater availability of vertebrate genomes)
206 confirm the wide distribution and early origin of Bcl-2 in Metazoa[11,32,48,50]. Proteins clustered
207 into five monophyletic groups, consistent with classical functional Bcl-2 classification (i.e.
208 three 'pro-apoptotic' clades: Bok, Bak, Bax and two less supported pro-survival - 'anti-
209 apoptotic' - groups: Bcl-2/W/XL and a more complex Bcl-B/Mcl-1/Bfl-1 clade) (Figure S5).
210 However, relationships among the five well-supported groups were not clearly resolved

211 despite the use of various methodologies and outgroup selections (Figure S5A-B).
212 Consequently, each of the five Bcl-2 clades seems conserved across evolution, and homology
213 (orthology) relationships inside each clade can be established. However, due to the
214 impossibility of addressing the relationship between these five monophyletic groups (Bok, Bak,
215 Bax, Bcl-2/W/XL, Bcl-B/Mcl-1/Bfl-1), it seems difficult to hypothesises their evolutionary
216 pattern, history, and determine a potential ancestral group. In addition, very divergent
217 sequences from molluscs such as *Biomphalaria glabrata* (Bcl-like2, Bcl-like3), from the
218 cnidarian *Hydra vulgaris* (Bcl-like1) or from the urochordate *Ciona intestinalis* (Bcl-like1) were
219 not assigned to a particular class.

220 *Caenorhabditis* is deprived of pro-apoptotic Bcl-2 and possesses only the pro-survival
221 Ced-9 (homolog to vertebrates Bcl-2/w/xl), and two BH-3 only proteins (Egl-1 and Ced-13).
222 Conversely, only two pro-apoptotic Bok-like paralogs (Debcl and Buffy) were present in
223 *Drosophila* (Figure 2, Figure S5), but their functions remain unclear[51]. Presence of both anti-
224 and pro-apoptotic Bcl-2 in molluscs underlines the divergent particularities observed within
225 protostomes. Contrarily, similarities in Bcl-2 family composition are observed within some
226 deuterostomes (mammals and echinoderms).

227 Finally, if multiple Bcl-2 genes were acquired early in metazoan evolution, and despite
228 conservation of almost homologous genes, key differences accumulate, making initiation
229 mechanisms in intrinsic apoptotic signalling pathways divergent among animals.

230

231 **Apoptotic mitochondrial pathways are divergent among metazoans**

232 Functional evidence shows that caspase-2 members play a critical role in various cell
233 death processes, but are independently involved in a range of non-apoptotic functions,
234 including cell cycle regulation, DNA repair and tumour suppression[52–55]. This implication of

235 caspase-2 in a myriad of signalling pathways, and its ability to interact with a panel of
236 molecules, demonstrates its functional versatility[52,53,56–59]. As previously reported, our
237 phylogenetic analyses corroborate the wide distribution of caspase-2 in bilaterians and
238 suggest a probable ancestral multifunctionality.

239 The major structural and functional similarities that led to an erroneous interpretation
240 of the phylogenetic position of Ced-3 and Dronc underlies a probable common evolutionary
241 origin of caspase-2 and -9 genes. We hypothesised here that caspase-9 originates from
242 bilaterians-specific duplication of a caspase-like ancestor gene, followed by a loss of caspase-
243 9 in protostomians (Figure 2). Among deuterostomians the two families of paralogs have been
244 preserved in vertebrates and probably in cephalochordates (Figure 1, 2). Caspase-2 retains
245 multifunctional activity, and in mammals can interact with the PIDDosome platform
246 containing P53, adapter molecule RAIDD, and signalling complex DISC, activating both
247 extrinsic and intrinsic apoptosis, and DNA damage pathways[58,60–62]. Conversely, the caspase-
248 9 gene underwent a functional divergence in connection with its specialisation in allosteric
249 interactions with the apoptosome[18].

250 Due to its pivotal role as a mediator of genomic stability through involvement in cell
251 proliferation, oxidative stress, aging and cell death, the molecular divergence of the caspase-
252 2 gene is highly constrained during evolution, probably because destabilisation of any
253 signalling cascade is sufficient to initiate tumorigenesis. Indeed, purifying selection is likely
254 important during caspase-2 evolution as illustrated by a dN/dS close to 0 (model M0 $\omega\theta$ =
255 0.07)[63,64]. However, during the radiation of deuterostomes, both presence of caspase-2 and -
256 9 certainly facilitated the loss of one of them (cf. DCC Force's model -Duplication-
257 Degeneration-Complementation model)[65–67]. Interestingly, a caspase-2 duplication co-
258 occurred with the loss of caspase-9 in urochordates that may indicate a clade-specific

259 relaxation of purifying selection on caspase-2 gene (Figure 1, Figure 2). Similarly, caspase-2
260 has been lost, or strongly diverged, while caspase-9 presents a *de novo* relative expansion in
261 *Strongylocentrotus purpuratus* (Echinodermata) and *Saccoglossus kowalevskii*
262 (Hemichordata). These expansions certainly result from a less powerful purifying selection of
263 caspase-9, showing a higher dN/dS (model M0 $\omega\theta = 0.22$) than caspase-2.

264 Due to generalised gene losses in ecdysozoans and in comparison with other
265 bilaterians, *Caenorhabditis* and *Drosophila* apoptotic pathways are generally considered
266 simpler than those of vertebrates[17,68]. However, comparing to mammals, ecdysozoans have
267 pathways organised around different paralogous genes in addition to a smaller number of
268 genes present. The absence of orthologous genes relationships results in a very different
269 structural organisation of apoptosome platforms but also generates important functional
270 divergences (i.e. mechanisms of regulating assembly, CARD-CARD interactions with
271 procaspases)[10].

272 Consistent with mammalian caspase-2 functions, Ced-3 has both initiator as well as
273 executioner activities[58,69–71]. Involvement of Dronc in various processes such as compensatory
274 cell proliferation, inhibition of cell migration or spermatid differentiation, brings this protein
275 closer to the functionalities of mammalian caspase-2[72,73]. Due to its interaction with Dark
276 (Apaf-1 paralog), the only CARD-caspase in *Drosophila* (Dronc) has been erroneously classified
277 as caspase-9[8,74]. Unlike the organisation of the mammal apoptosome, both *Caenorhabditis*
278 and *Drosophila* present neither MOMP nor the release and necessity of cytochrome c to
279 activate Ced-3 and Dronc via Ced-4 and Dark, respectively[5,68].

280 Like other protostomes, molluscs are devoid of caspase-9 but caspase-2 has been
281 identified in bivalves and was suspected to function in "a caspase-9-like manner"[75]. Hence,
282 caspase-2 seems involved in apoptotic processes in molluscs, but more surprisingly, despite

283 the absence of caspase-9 and Apaf-1 (and thus, of a mammalian-like apoptosome), this
284 peculiar pathway is surprisingly associated with cytochrome c release[38,41,76–79]. The complexity
285 of intrinsic apoptosis in molluscs seems to be important, but divergent from what was
286 observed in ecdysozoans or vertebrates, with a putative expansion of caspases that
287 participate both in immunity, stress responses, and apoptosis (Figure 2)[41,75,80–83].

288 Unexpectedly, mammals present an almost unique case (possibly with the
289 cephalochordates) in which both caspase-2 and caspase-9 are conserved and involved in
290 apoptosis. This putative functional redundancy (i.e. recruitment, autoactivation or
291 transactivation, homodimerisation and subsequent interchain proteolytic cleavage)
292 undoubtedly led to the functional specialisation observed for caspase-9. This may results from
293 the specificity of the mammalian mitochondrial pathway and the non-apoptotic function of
294 caspase-9[84–87]. Finally, echinoderms seem to uniquely have an intrinsic apoptosis similar to
295 mammals, with a caspase-9, Bcl-2, Apaf-1, and a MOMP with cytochrome c release (Figure
296 2)[7,88].

297 Although we can envisage a weak parsimonious scenario that showcases a common
298 ancestral apoptotic pathway in deuterostomes (but implying independent secondary losses in
299 hemichordates, cephalocordates, and urochordates), the similarities observed between
300 echinoderms and mammals more probably reflect "functional convergences" based on
301 independent recruitment of apoptotic actors.

302

303 **CONCLUSION**

304 The apoptotic networks of *Caenorhabditis* and *Drosophila* do not exemplify ancestral
305 conditions from which mammalian-grade apoptotic complexity emerged but are on the

306 contrary, and as suggested recently, the result of a derived condition specific to ecdysozoans
307 among animals [32,80,89,90].

308 The core components of intrinsic apoptotic pathways, especially initiator caspases and
309 the apoptosome platform, are not ancestral in metazoans. Our phylogenetic analyses highlight
310 an unexpected evolutionary history: while the bilaterian caspase-2-mediated apoptotic toolkit
311 emerged ancestrally and remains multifunctional, the caspase-9 mediator of the mammalian
312 apoptosome is specific to deuterostomes.

313 The major functional divergences in mitochondrial apoptotic pathways observed in
314 animals[70,91–93] mainly originated in the recruitment of paralogous actors from the same
315 multigenic families. The evolution of the different pathways underlined by non-homologous
316 molecular actors could be the reflection of putative adaptive processes or constrains specific
317 to each taxon, which ultimately led to divergent evolutionary histories. Interestingly, the
318 richness of the apoptotic genetic repertoire was suggested to be linked to the persistence of
319 stem cells in adults from different phyla[94,95].

320 Finally, mitochondria-mediated apoptosis, like other programmed cell deaths, has
321 likely evolved before and throughout metazoan diversification to shape developmental
322 processes, immune response, or to adapt cellular environment to environmental constraint.

323

324 **MATERIAL AND METHODS**

325 **Sequence dataset construction**

326 Putative metazoan caspases with a CARD pro-domain (CARD-caspases) were identified
327 using tBLASTn and BLASTp searches with human caspases, Ced-3, and Dronc as queries on
328 NCBI, ANISEED (ascidians), EchinoBase (*Strongylocentrotus purpuratus*), and
329 neurobase.rc.ufl.edu (*Pleurobrachia bachei*) databases, and followed by reciprocal BLAST.

330 After identification of CARD-caspases in target species, sequences were added as queries to
331 conduct BLAST searches in close relatives (i.e. identified CARD-caspases of *Crassostrea gigas*
332 were used as queries to search in other molluscs). Genomes and transcriptomes of species'
333 were downloaded when possible, to search a second time. Sequences with an e-value inferior
334 to 1e-10 were retained. All identified sequences were analysed with ScanProsite (ExPaSy)[96]
335 and InterProScan (EMBL-EBI)[97] to verify the presence of specific caspase domains. Another
336 sequence was added to verify its identification proposed as a caspase-2 in the literature:
337 *Crassostrea angulata* caspase-2[79]. Caspase family proteins are short (containing the large
338 common P20 and the small P10 domains) with a high number of genes per species which
339 rapidly limits the relevance of the phylogenetic analyses. To reduce artefact branching and
340 unreadable topologies, and to maximize phylogenetic diversity across Metazoa, the dataset
341 was built using CARD-caspase gene repertoires of selected species. A full list of all caspase
342 sequences is provided in Table S1. Taxon and genes were selected to have a wide diversity of
343 major metazoan phyla and to have an equilibrium inside and between each group. We choose
344 representative species for each phylum and took care to don't unreasonably increase the
345 number of sequences by redundant choice. We privileged species where we detected
346 caspases with CARD domains, DED domains, and executioner caspases, suggesting a high
347 quality of sequences allowing identification of all members of the caspase family. For each
348 taxon, all caspases having a CARD pro-domains have been include in the analysis.

349 Identification of metazoan Apaf-1 was made using tBLASTn and BLASTp using human
350 APAF-1, nematode Ced-4, and fly Dark as queries on NCBI, ANISEED (ascidians), and
351 neurobase.rc.ufl.edu (*Pleurobrachia bachei*) databases, and followed by reciprocal BLAST.
352 Potential resulting sequences were analysed with ScanProsite and also InterProScan. A full list

353 of all Apaf-1 sequences is provided in Table S4. Apaf-1 data set comprise sequences from a
354 previous study[33] in addition to our new sequences.

355 Metazoan Bcl-2 were identified by using tBLASTn and BLASTp searches with human
356 Bcl-2 as the query sequence on NCBI, and then again on downloaded genomes and
357 transcriptomes, followed by reciprocal BLAST. All identified sequences were analysed with
358 ScanProsite (ExPaSy) and InterProScan (EMBL-EBI) to verify the presence of BH domains. Due
359 to short sequence length, BH3-only were not taken into account. A full list of all Bcl-2
360 sequences is provided in Table S5.

361 Multiple alignments of protein sequences were generated using the MAFFT software
362 version 7[98] with default parameters and also Clustal Omega[99] to verify the congruence of the
363 different alignments. All sequences were then manually checked in BioEdit 7.2 software[100] to
364 verify the presence of specific domains previously identified. Gblocks version 0.91b[101] was
365 used to remove vacancies and blur sites. Final alignments comprise of 230, 235, 147, and 306
366 amino acids for metazoan CARD-caspases alignment, deuterostomian CARD-caspases
367 alignment, metazoan Bcl-2 alignment, and Apaf-1 alignment, respectively. Apaf-1 alignment
368 was done on the NB-ARC domain only.

369

370 **Phylogenetic analysis**

371 Phylogenetic analyses were carried out from the amino-acid alignment with
372 Maximum-Likelihood (ML) method in PhyML 3.1[102], a combined ML tree search with 1000
373 bootstrap replicates was produced and then visualised using Seaview[103]. The best amino-acid
374 evolution models to conduct analyses were determined using MEGA11[104] and determined to
375 be WAG for sequences of CARD-caspases alignments (CARD, P20, P10) and LG for both Bcl-2
376 and Apaf-1 alignments.

377 Bayesian analyses were performed using MrBayes (v3.2.6)[105] under mixed model. For
378 each analysis, one fourth of the topologies were discarded as burn-in values, while the
379 remaining ones were used to calculate posterior probability. The run for metazoan CARD-
380 caspases alignment were carried out for 2,000,000 generations with 15 randomly started
381 simultaneous Markov chains (1 cold chain, 14 heated chains) and sampled every 100
382 generations. The run for deuterostomian CARD-caspases alignment was carried out for
383 500,000 generations with 5 randomly started simultaneous Markov chains (1 cold chain, 4
384 heated chains) and sampled every 100 generations. The run for metazoan Apaf-1 alignment
385 was carried out for 500,000 generations with 5 randomly started simultaneous Markov chains
386 (1 cold chain, 4 heated chains) and sampled every 100 generations. The run for metazoan Bcl-
387 2 alignment was carried out for 5,000,000 generations with 20 randomly started simultaneous
388 Markov chains (1 cold chain, 19 heated chains) and sampled every 100 generations. ML
389 bootstrap values higher than 50% and Bayesian posterior probabilities are indicated on the
390 Bayesian tree.

391 The outgroup for the metazoan CARD-caspase phylogeny is the only caspase with a
392 CARD pro-domain of the Porifera *Amphimedon queenslandica* (XP_003383519) (Figure 1, S4,
393 S5) or the only one of the ctenophore *Pleurobrachia bachei* (Sb 2658116) (Figure S2). Analyses
394 of CARD-caspases were made independently at the deuterostome scale with four different
395 outgroups to test their effect on the stability of the topology: *i*) CARD-caspase-Y of the annelid
396 *Capitella teleta* (ELT97848.1), *ii*) CARD-caspase-2 of the mollusk *Aplysia californica*
397 (XP_005113266), *iii*) CARD-caspase-X2 of cnidarian *Hydra vulgaris* (NP_001274285.1) *iv*)
398 CARD-caspase Ced-3 of the ecdysozoan *Caenorhabditis elegans* (AAG42045.1) (Figure S3). For
399 the metazoan Apaf-1 phylogenies, the selected outgroup is Apaf-1 (XP_019855714.1) of
400 Porifera *Amphimedon queenslandica* (Figure S4). For the metazoan Bcl-2 phylogenies,

outgroups used to test their effect on stability of the topology are: *i*) Bcl-2-like1 (XP_003383425.1) and Bcl-2-like2 (XP_003387574.1) of Porifera *Amphimedon queenslandica* (Figure S5).

Topology tests between metazoan CARD-caspase phylogenies from Bayesian inference method and maximum likelihood estimation were evaluated using IQ-TREE[106]. We conducted Kishino-Hasegawa test[107], Shimodaira-Hasegawa test, and approximately unbiased test[108].

Estimation of dN/dS and recombination rate

Codon aligned nucleotide sequences were built using PAL2NAL[109] from clustalo aligned amino acid sequences and gene ORFs. The dN/dS ratio was calculated using EasyCodeML under settings "site model", nuc-2, and standard icode[64], from the codon aligned nucleotide sequences and newick format trees.

Co-estimation of recombination rate was conducted using ProteinEvolverABC[29]. We run the analysis on the same multiple protein alignment we used for the metazoan CARD-caspases phylogenetic analysis, including CARD, P20, and P10 domains. Analysis was conducted with 10 000 simulations and an acceptance rate of 0.2% to optimise the accuracy of the estimations (Beaumont 2010), and under WAG amino acid substitution model. Prior parameters were estimated by ProteinEvolverABC prior to the analysis such as Rho = Uniform (0, $3.0e^{-6}$) and Theta = Uniform ($9.1e^{-5}$, $4.0e^{-4}$). Proportion of invariable sites was 0.026 and amino acid frequencies were fix.

Acknowledgements

Authors particularly acknowledge Helen R Horkan (University of Galway, Ireland) for help in bioinformatics analysis and helpful comments, and Miguel Arenas (University of Vigo, Spain) for discussion and assistance with ProteinEvolverABC. Authors thank Sébastien Darras (Sorbonne Université, Banyuls-sur-Mer), Christine Vesque (Sorbonne Université, Paris), Jérôme Gros (Institut Pasteur, Paris), Sabine Hennequin (Sorbonne Université, Paris) and Uri Frank (University of Galway, Ireland) for helpful comments. GK was supported by a Ph.D. fellowship from the French Ministry of Education, Research and Innovation.

Author Contributions

JP and EQ managed the project. GK made BLAST, phylogenetic and sequences analysis, and figures. GK and EQ wrote the manuscript.

Competing Interest Statement

The authors declare no competing interests.

Data Availability

All data needed to evaluate the conclusions in this study are present in the paper and the Supplementary Materials. Any requests can be addressed to the corresponding author.

446

447 **BIBLIOGRAPHY**

448 1. Jacobson, M. D., Weil, M. & Raff, M. C. Programmed cell death in animal development. *Cell* **88**,
449 347–354 (1997).
450 2. Hipfner, D. R. & Cohen, S. M. Connecting proliferation and apoptosis in development and
451 disease. *Nat Rev Mol Cell Biol* **5**, 805–815 (2004).
452 3. Vriz, S., Reiter, S. & Galliot, B. Cell death: a program to regenerate. *Curr. Top. Dev. Biol.* **108**, 121–
453 151 (2014).
454 4. Hengartner, M. O. The biochemistry of apoptosis. *Nature* **407**, 770–776 (2000).
455 5. Lettre, G. & Hengartner, M. O. Developmental apoptosis in C. elegans: a complex CEDnario. *Nat*
456 *Rev Mol Cell Biol* **7**, 97–108 (2006).
457 6. Ellis, H. M. & Horvitz, H. R. Genetic control of programmed cell death in the nematode C.
458 elegans. *Cell* **44**, 817–829 (1986).
459 7. Bender, C. E. *et al.* Mitochondrial pathway of apoptosis is ancestral in metazoans. *Proc. Natl.*
460 *Acad. Sci. U.S.A.* **109**, 4904–4909 (2012).
461 8. Steller, H. Regulation of apoptosis in Drosophila. *Cell Death Differ.* **15**, 1132–1138 (2008).
462 9. Driscoll, M. Cell death in C. elegans: molecular insights into mechanisms conserved between
463 nematodes and mammals. *Brain Pathol* **6**, 411–425 (1996).
464 10. Dorstyn, L., Akey, C. W. & Kumar, S. New insights into apoptosome structure and function. *Cell*
465 *Death Differ* **25**, 1194–1208 (2018).
466 11. Young, N. D. *et al.* Diversity in the intrinsic apoptosis pathway of nematodes. *Commun Biol* **3**, 478
467 (2020).
468 12. Bell, R. A. V. & Megeney, L. A. Evolution of caspase-mediated cell death and differentiation:
469 twins separated at birth. *Cell Death Differ* **24**, 1359–1368 (2017).
470 13. Shrestha, S. *et al.* Caspases from scleractinian coral show unique regulatory features. *J Biol Chem*
471 **295**, 14578–14591 (2020).

472 14. Uren, A. G. *et al.* Identification of Paracaspases and Metacaspases: Two Ancient Families of
473 Caspase-like Proteins, One of which Plays a Key Role in MALT Lymphoma. *Molecular Cell* **6**, 961–
474 967 (2000).
475 15. Crawford, E. D. *et al.* Conservation of caspase substrates across metazoans suggests hierarchical
476 importance of signaling pathways over specific targets and cleavage site motifs in apoptosis. *Cell*
477 *Death Differ* **19**, 2040–2048 (2012).
478 16. Thornberry, N. A. & Lazebnik, Y. Caspases: enemies within. *Science* **281**, 1312–1316 (1998).
479 17. S, E. Apoptosis: a review of programmed cell death. *Toxicologic pathology* vol. 35
480 https://pubmed.ncbi.nlm.nih.gov/17562483/ (2007).
481 18. Galluzzi, L. *et al.* Molecular mechanisms of cell death: recommendations of the Nomenclature
482 Committee on Cell Death 2018. *Cell Death Differ.* **25**, 486–541 (2018).
483 19. Terajima, D. *et al.* Identification of candidate genes encoding the core components of the cell
484 death machinery in the Ciona intestinalis genome. *Cell Death Differ.* **10**, 749–753 (2003).
485 20. Delsuc, F., Brinkmann, H., Chourrout, D. & Philippe, H. Tunicates and not cephalochordates are
486 the closest living relatives of vertebrates. *Nature* **439**, 965–968 (2006).
487 21. Lee, T. V., Kamber Kaya, H. E., Simin, R., Baehrecke, E. H. & Bergmann, A. The initiator caspase
488 Dronc is subject of enhanced autophagy upon proteasome impairment in Drosophila. *Cell Death*
489 *Differ* **23**, 1555–1564 (2016).
490 22. Fogarty, C. E. *et al.* Extracellular Reactive Oxygen Species Drive Apoptosis-Induced Proliferation
491 via Drosophila Macrophages. *Curr Biol* **26**, 575–584 (2016).
492 23. Fan, Y. *et al.* Genetic models of apoptosis-induced proliferation decipher activation of JNK and
493 identify a requirement of EGFR signaling for tissue regenerative responses in Drosophila. *PLoS*
494 *Genet* **10**, e1004131 (2014).
495 24. Fan, Y. & Bergmann, A. The cleaved-Caspase-3 antibody is a marker of Caspase-9-like DRONC
496 activity in Drosophila. *Cell Death Differ* **17**, 534–539 (2010).
497 25. Napoletano, F. *et al.* p53-dependent programmed necrosis controls germ cell homeostasis
498 during spermatogenesis. *PLoS Genet* **13**, e1007024 (2017).
499 26. Lim, Y., Dorstyn, L. & Kumar, S. The p53-caspase-2 axis in the cell cycle and DNA damage
500 response. *Exp Mol Med* **53**, 517–527 (2021).

501 27. Bao, Q. & Shi, Y. Apoptosome: a platform for the activation of initiator caspases. *Cell Death Differ*
502 **14**, 56–65 (2007).
503 28. Jaroszewski, L., Rychlewski, L., Reed, J. C. & Godzik, A. ATP-activated oligomerization as a
504 mechanism for apoptosis regulation: fold and mechanism prediction for CED-4. *Proteins* **39**, 197–
505 203 (2000).
506 29. Arenas, M. ProteinEvolverABC: Coestimation of Recombination and Substitution Rates in Protein
507 Sequences by approximate Bayesian computation. *Bioinformatics* btab617 (2021)
508 doi:10.1093/bioinformatics/btab617.
509 30. Lulla, V. & Firth, A. E. A hidden gene in astroviruses encodes a viroporin. *Nat Commun* **11**, 4070
510 (2020).
511 31. Nieva, J. L., Madan, V. & Carrasco, L. Viroporins: structure and biological functions. *Nat Rev*
512 *Microbiol* **10**, 563–574 (2012).
513 32. Zmasek, C. M. & Godzik, A. Evolution of the animal apoptosis network. *Cold Spring Harb Perspect*
514 *Biol* **5**, a008649 (2013).
515 33. Zmasek, C. M., Zhang, Q., Ye, Y. & Godzik, A. Surprising complexity of the ancestral apoptosis
516 network. *Genome Biol.* **8**, R226 (2007).
517 34. Zou, H., Henzel, W. J., Liu, X., Lutschg, A. & Wang, X. Apaf-1, a human protein homologous to C.
518 elegans CED-4, participates in cytochrome c-dependent activation of caspase-3. *Cell* **90**, 405–413
519 (1997).
520 35. Zou, H., Li, Y., Liu, X. & Wang, X. An APAF-1.cytochrome c multimeric complex is a functional
521 apoptosome that activates procaspase-9. *J. Biol. Chem.* **274**, 11549–11556 (1999).
522 36. Dorstyn, L. *et al.* The role of cytochrome c in caspase activation in Drosophila melanogaster cells.
523 *J Cell Biol* **156**, 1089–1098 (2002).
524 37. Shi, Y. Mechanical aspects of apoptosome assembly. *Curr Opin Cell Biol* **18**, 677–684 (2006).
525 38. Li, Y. *et al.* Conservation and divergence of mitochondrial apoptosis pathway in the Pacific oyster,
526 Crassostrea gigas. *Cell Death Dis* **8**, e2915 (2017).
527 39. Kiss, T. Apoptosis and its functional significance in molluscs. *Apoptosis* **15**, 313–321 (2010).
528 40. Romero, A., Novoa, B. & Figueras, A. The complexity of apoptotic cell death in mollusks: An
529 update. *Fish Shellfish Immunol.* **46**, 79–87 (2015).

530 41. Estévez-Calvar, N., Romero, A., Figueras, A. & Novoa, B. Genes of the mitochondrial apoptotic
531 pathway in Mytilus galloprovincialis. *PLoS ONE* **8**, e61502 (2013).
532 42. Srivastava, M. *et al.* The Amphimedon queenslandica genome and the evolution of animal
533 complexity. *Nature* **466**, 720–726 (2010).
534 43. Srivastava, M. *et al.* The Trichoplax genome and the nature of placozoans. *Nature* **454**, 955–960
535 (2008).
536 44. Zermati, Y. *et al.* Nonapoptotic role for Apaf-1 in the DNA damage checkpoint. *Mol Cell* **28**, 624–
537 637 (2007).
538 45. Ferraro, E. *et al.* Apaf1 plays a pro-survival role by regulating centrosome morphology and
539 function. *J Cell Sci* **124**, 3450–3463 (2011).
540 46. Shakeri, R., Kheirollahi, A. & Davoodi, J. Apaf-1: Regulation and function in cell death. *Biochimie*
541 **135**, 111–125 (2017).
542 47. Lee, E. F. *et al.* Discovery and molecular characterization of a Bcl-2-regulated cell death pathway
543 in schistosomes. *Proc. Natl. Acad. Sci. U.S.A.* **108**, 6999–7003 (2011).
544 48. Banjara, S., Suraweera, C. D., Hinds, M. G. & Kvansakul, M. The Bcl-2 Family: Ancient Origins,
545 Conserved Structures, and Divergent Mechanisms. *Biomolecules* **10**, (2020).
546 49. Kalkavan, H. & Green, D. R. MOMP, cell suicide as a BCL-2 family business. *Cell Death Differ* **25**,
547 46–55 (2018).
548 50. Dunn, S. R., Phillips, W. S., Spatafora, J. W., Green, D. R. & Weis, V. M. Highly conserved caspase
549 and Bcl-2 homologues from the sea anemone Aiptasia pallida: lower metazoans as models for
550 the study of apoptosis evolution. *J. Mol. Evol.* **63**, 95–107 (2006).
551 51. Clavier, A., Rincheval-Arnold, A., Colin, J., Mignotte, B. & Guénal, I. Apoptosis in Drosophila:
552 which role for mitochondria? *Apoptosis* **21**, 239–251 (2016).
553 52. Krumschnabel, G., Sohm, B., Bock, F., Manzl, C. & Villunger, A. The enigma of caspase-2: the
554 laymen's view. *Cell Death & Differentiation* **16**, 195–207 (2009).
555 53. Olsson, M., Forsberg, J. & Zhivotovsky, B. Caspase-2: the reinvented enzyme. *Oncogene* **34**,
556 1877–1882 (2015).
557 54. Lassus, P., Opitz-Araya, X. & Lazebnik, Y. Requirement for caspase-2 in stress-induced apoptosis
558 before mitochondrial permeabilization. *Science* **297**, 1352–1354 (2002).

559 55. Zhivotovsky, B. & Orrenius, S. Caspase-2 function in response to DNA damage. *Biochem. Biophys.*
560 *Res. Commun.* **331**, 859–867 (2005).
561 56. Krumschnabel, G., Manzl, C. & Villunger, A. Caspase-2: killer, savior and safeguard--emerging
562 versatile roles for an ill-defined caspase. *Oncogene* **28**, 3093–3096 (2009).
563 57. Olsson, M. *et al.* DISC-mediated activation of caspase-2 in DNA damage-induced apoptosis.
564 *Oncogene* **28**, 1949–1959 (2009).
565 58. Lavrik, I. N., Golks, A., Baumann, S. & Krammer, P. H. Caspase-2 is activated at the CD95 death-
566 inducing signaling complex in the course of CD95-induced apoptosis. *Blood* **108**, 559–565 (2006).
567 59. Braga, M. *et al.* Involvement of oxidative stress and caspase 2-mediated intrinsic pathway
568 signaling in age-related increase in muscle cell apoptosis in mice. *Apoptosis* **13**, 822–832 (2008).
569 60. Duan, H. & Dixit, V. M. RAIDD is a new 'death' adaptor molecule. *Nature* **385**, 86–89 (1997).
570 61. Tinel, A. & Tschopp, J. The PIDDosome, a protein complex implicated in activation of caspase-2 in
571 response to genotoxic stress. *Science* **304**, 843–846 (2004).
572 62. Haupt, S., Berger, M., Goldberg, Z. & Haupt, Y. Apoptosis - the p53 network. *J Cell Sci* **116**, 4077–
573 4085 (2003).
574 63. Eyre-Walker, A. The genomic rate of adaptive evolution. *Trends Ecol Evol* **21**, 569–575 (2006).
575 64. Gao, F. *et al.* EasyCodeML: A visual tool for analysis of selection using CodeML. *Ecol Evol* **9**, 3891–
576 3898 (2019).
577 65. Force, A. *et al.* Preservation of duplicate genes by complementary, degenerative mutations.
578 *Genetics* **151**, 1531–1545 (1999).
579 66. Conant, G. C. & Wolfe, K. H. Turning a hobby into a job: how duplicated genes find new
580 functions. *Nat Rev Genet* **9**, 938–950 (2008).
581 67. Fares, M. A., Keane, O. M., Toft, C., Carretero-Paulet, L. & Jones, G. W. The roles of whole-
582 genome and small-scale duplications in the functional specialization of Saccharomyces cerevisiae
583 genes. *PLoS Genet* **9**, e1003176 (2013).
584 68. Meier, P., Finch, A. & Evan, G. Apoptosis in development. *Nature* **407**, 796–801 (2000).
585 69. Degterev, A., Boyce, M. & Yuan, J. A decade of caspases. *Oncogene* **22**, 8543–8567 (2003).
586 70. Fuchs, Y. & Steller, H. Live to die another way: modes of programmed cell death and the signals
587 emanating from dying cells. *Nat. Rev. Mol. Cell Biol.* **16**, 329–344 (2015).

588 71. Mancini, M. *et al.* Caspase-2 Is Localized at the Golgi Complex and Cleaves Golgin-160 during
589 Apoptosis. *J Cell Biol* **149**, 603–612 (2000).
590 72. Ouyang, Y. *et al.* Dronc caspase exerts a non-apoptotic function to restrain phospho-Numb-
591 induced ectopic neuroblast formation in Drosophila. *Development* **138**, 2185–2196 (2011).
592 73. Huh, J. R., Guo, M. & Hay, B. A. Compensatory proliferation induced by cell death in the
593 Drosophila wing disc requires activity of the apical cell death caspase Dronc in a nonapoptotic
594 role. *Curr. Biol.* **14**, 1262–1266 (2004).
595 74. Kumar, S. & Doumanis, J. The fly caspases. *Cell Death Differ* **7**, 1039–1044 (2000).
596 75. Vogeler, S., Carboni, S., Li, X. & Joyce, A. Phylogenetic analysis of the caspase family in bivalves:
597 implications for programmed cell death, immune response and development. *BMC Genomics* **22**,
598 80 (2021).
599 76. Pirger, Z., Rácz, B. & Kiss, T. Dopamine-induced programmed cell death is associated with
600 cytochrome c release and caspase-3 activation in snail salivary gland cells. *Biol. Cell* **101**, 105–116
601 (2009).
602 77. Romero, A., Estévez-Calvar, N., Dios, S., Figueras, A. & Novoa, B. New insights into the apoptotic
603 process in mollusks: characterization of caspase genes in Mytilus galloprovincialis. *PLoS ONE* **6**,
604 e17003 (2011).
605 78. Zhang, L., Li, L. & Zhang, G. Gene discovery, comparative analysis and expression profile reveal
606 the complexity of the Crassostrea gigas apoptosis system. *Dev. Comp. Immunol.* **35**, 603–610
607 (2011).
608 79. Yang, B. *et al.* Molecular cloning of two molluscan caspases and gene functional analysis during
609 Crassostrea angulata (Fujian oyster) larval metamorphosis. *Mol. Biol. Rep.* **42**, 963–975 (2015).
610 80. Plachetzki, D. C., Pankey, M. S., MacManes, M. D., Lesser, M. P. & Walker, C. W. The Genome of
611 the Softshell Clam Mya arenaria and the Evolution of Apoptosis. *Genome Biol Evol* **12**, 1681–
612 1693 (2020).
613 81. Piquet, B., Shillito, B., Lallier, F. H., Duperron, S. & Andersen, A. C. High rates of apoptosis
614 visualized in the symbiont-bearing gills of deep-sea Bathymodiolus mussels. *PLoS ONE* **14**,
615 e0211499 (2019).

616 82. Sokolova, I. M., Evans, S. & Hughes, F. M. Cadmium-induced apoptosis in oyster hemocytes
617 involves disturbance of cellular energy balance but no mitochondrial permeability transition. *J.*
618 *Exp. Biol.* **207**, 3369–3380 (2004).
619 83. Sokolova, I. M. Apoptosis in molluscan immune defense. *Invertebrate Survival Journal* **6**, 49–58
620 (2009).
621 84. An, H.-K. *et al.* CASP9 (caspase 9) is essential for autophagosome maturation through regulation
622 of mitochondrial homeostasis. *Autophagy* **16**, 1598–1617 (2020).
623 85. Madadi, Z., Akbari-Birgani, S., Monfared, P. D. & Mohammadi, S. The non-apoptotic role of
624 caspase-9 promotes differentiation in leukemic cells. *Biochim Biophys Acta Mol Cell Res* **1866**,
625 118524 (2019).
626 86. Hollville, E. & Deshmukh, M. Physiological functions of non-apoptotic caspase activity in the
627 nervous system. *Semin Cell Dev Biol* **82**, 127–136 (2018).
628 87. Tran, H. T. *et al.* Caspase-9 has a nonapoptotic function in Xenopus embryonic primitive blood
629 formation. *J Cell Sci* **130**, 2371–2381 (2017).
630 88. Tamura, R. *et al.* Starfish Apaf-1 activates effector caspase-3/9 upon apoptosis of aged eggs. *Sci*
631 *Rep* **8**, 1611 (2018).
632 89. Belyi, V. A. *et al.* The origins and evolution of the p53 family of genes. *Cold Spring Harb Perspect*
633 *Biol* **2**, a001198 (2010).
634 90. Lu, W.-J., Amatruda, J. F. & Abrams, J. M. p53 ancestry: gazing through an evolutionary lens. *Nat*
635 *Rev Cancer* **9**, 758–762 (2009).
636 91. Berthelet, J. & Dubrez, L. Regulation of Apoptosis by Inhibitors of Apoptosis (IAPs). *Cells* **2**, 163–
637 187 (2013).
638 92. Ribeiro Lopes, M., Parisot, N., Callaerts, P. & Calevro, F. Genetic Diversity of the Apoptotic
639 Pathway in Insects. in *Evolution, Origin of Life, Concepts and Methods* (ed. Pontarotti, P.) 253–
640 285 (Springer International Publishing, 2019). doi:10.1007/978-3-030-30363-1_13.
641 93. Ribeiro Lopes, M. *et al.* Evolutionary novelty in the apoptotic pathway of aphids. *Proc Natl Acad*
642 *Sci U S A* **117**, 32545–32556 (2020).
643 94. Aubrey, B. J. *et al.* Mutant TRP53 exerts a target gene-selective dominant-negative effect to drive
644 tumor development. *Genes Dev* **32**, 1420–1429 (2018).

645 95. Aubrey, B. J., Kelly, G. L., Janic, A., Herold, M. J. & Strasser, A. How does p53 induce apoptosis
646 and how does this relate to p53-mediated tumour suppression? *Cell Death Differ* **25**, 104–113
647 (2018).
648 96. Gattiker, A., Gasteiger, E. & Bairoch, A. ScanProsite: a reference implementation of a PROSITE
649 scanning tool. *Appl Bioinformatics* **1**, 107–108 (2002).
650 97. Quevillon, E. *et al.* InterProScan: protein domains identifier. *Nucleic Acids Res* **33**, W116-120
651 (2005).
652 98. Katoh, K. & Standley, D. M. MAFFT multiple sequence alignment software version 7:
653 improvements in performance and usability. *Mol. Biol. Evol.* **30**, 772–780 (2013).
654 99. Sievers, F. *et al.* Fast, scalable generation of high-quality protein multiple sequence alignments
655 using Clustal Omega. *Mol. Syst. Biol.* **7**, 539 (2011).
656 100. HALL, T. A. BioEdit : a user-friendly biological sequence alignment editor and analysis
657 program for Windows 95/98/NT. *Nucleic Acids Symp. Ser.* **41**, 95–98 (1999).
658 101. Castresana, J. Selection of conserved blocks from multiple alignments for their use in
659 phylogenetic analysis. *Mol. Biol. Evol.* **17**, 540–552 (2000).
660 102. Guindon, S. *et al.* New algorithms and methods to estimate maximum-likelihood phylogenies:
661 assessing the performance of PhyML 3.0. *Syst. Biol.* **59**, 307–321 (2010).
662 103. Gouy, M., Guindon, S. & Gascuel, O. SeaView version 4: A multiplatform graphical user
663 interface for sequence alignment and phylogenetic tree building. *Mol Biol Evol* **27**, 221–224
664 (2010).
665 104. Tamura, K., Stecher, G. & Kumar, S. MEGA11: Molecular Evolutionary Genetics Analysis
666 Version 11. *Mol Biol Evol* **38**, 3022–3027 (2021).
667 105. Ronquist, F. & Huelsenbeck, J. P. MrBayes 3: Bayesian phylogenetic inference under mixed
668 models. *Bioinformatics* **19**, 1572–1574 (2003).
669 106. Nguyen, L.-T., Schmidt, H. A., von Haeseler, A. & Minh, B. Q. IQ-TREE: A Fast and Effective
670 Stochastic Algorithm for Estimating Maximum-Likelihood Phylogenies. *Mol Biol Evol* **32**, 268–274
671 (2015).

107. Kishino, H. & Hasegawa, M. Evaluation of the maximum likelihood estimate of the evolutionary tree topologies from DNA sequence data, and the branching order in hominoidea. *J Mol Evol* **29**, 170–179 (1989).

108. Shimodaira, H. An approximately unbiased test of phylogenetic tree selection. *Syst Biol* **51**, 492–508 (2002).

109. Suyama, M., Torrents, D. & Bork, P. PAL2NAL: robust conversion of protein sequence alignments into the corresponding codon alignments. *Nucleic Acids Res* **34**, W609-612 (2006).

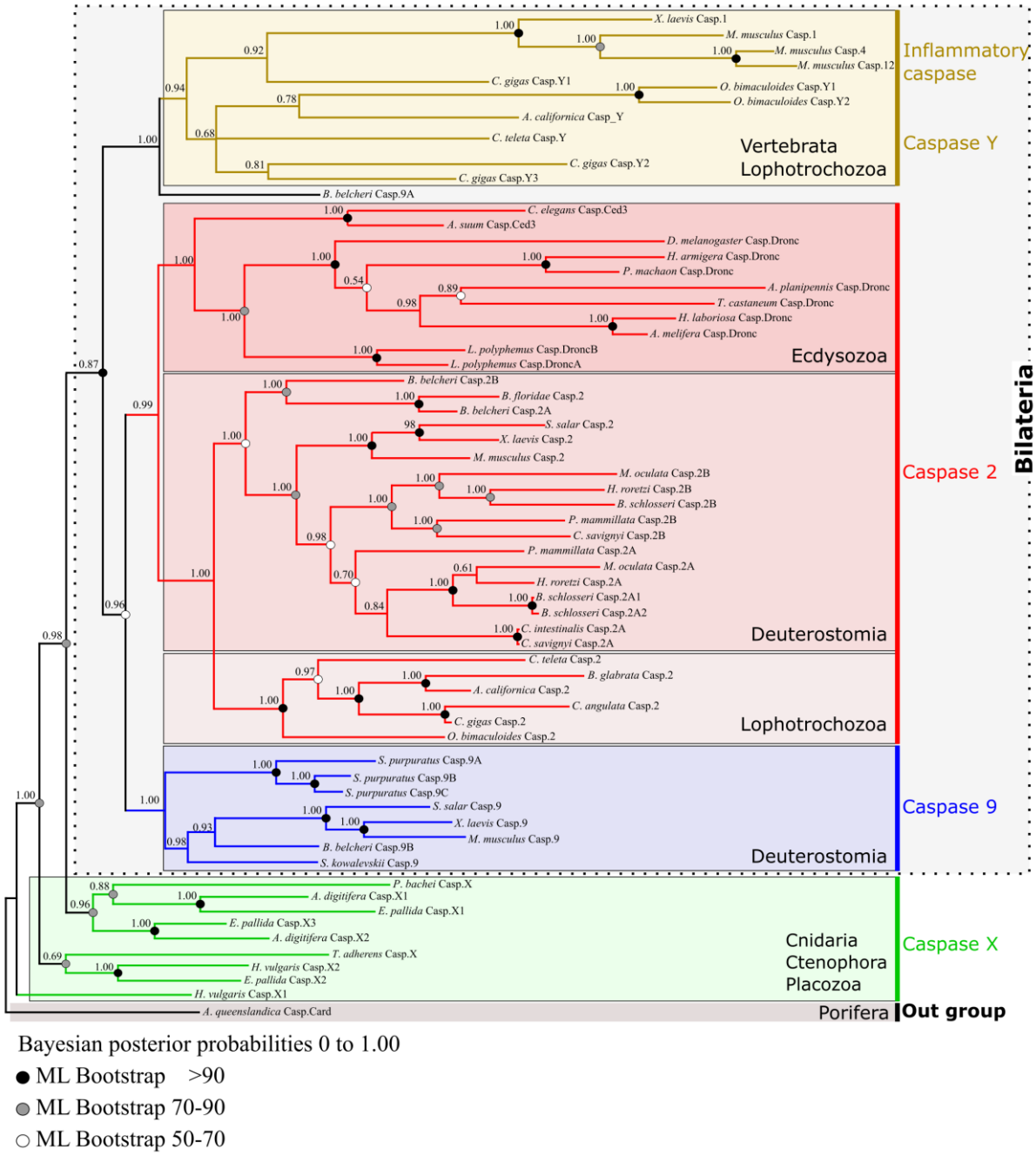

Figure 1:

Topology of metazoan CARD-caspase phylogeny obtained by Bayesian inference using full sequences alignment. Three strongly supported monophyletic groups are identified: caspase-9, caspase-2 and a more heterogeneous group named here [Inflammatory Caspases + Caspase-Y]. Together they form a clade strictly corresponding to bilaterian animals. Caspase-2 is widely distributed among bilaterians [Deutostomia + Ecdysozoa +

698 Lophotrochozoa/Spiralia] reflecting an ancestral origin. Conversely, caspase-9 is strictly
699 restricted to deuterostomian animals. Sequences of non-bilaterians (Cnidaria + Ctenophora +
700 Placozoa) form divergent paraphyletic groups. The selected outgroup is the unique CARD-
701 caspase of Porifera *Amphimedon queenslandica*.

702

703

704

705

706

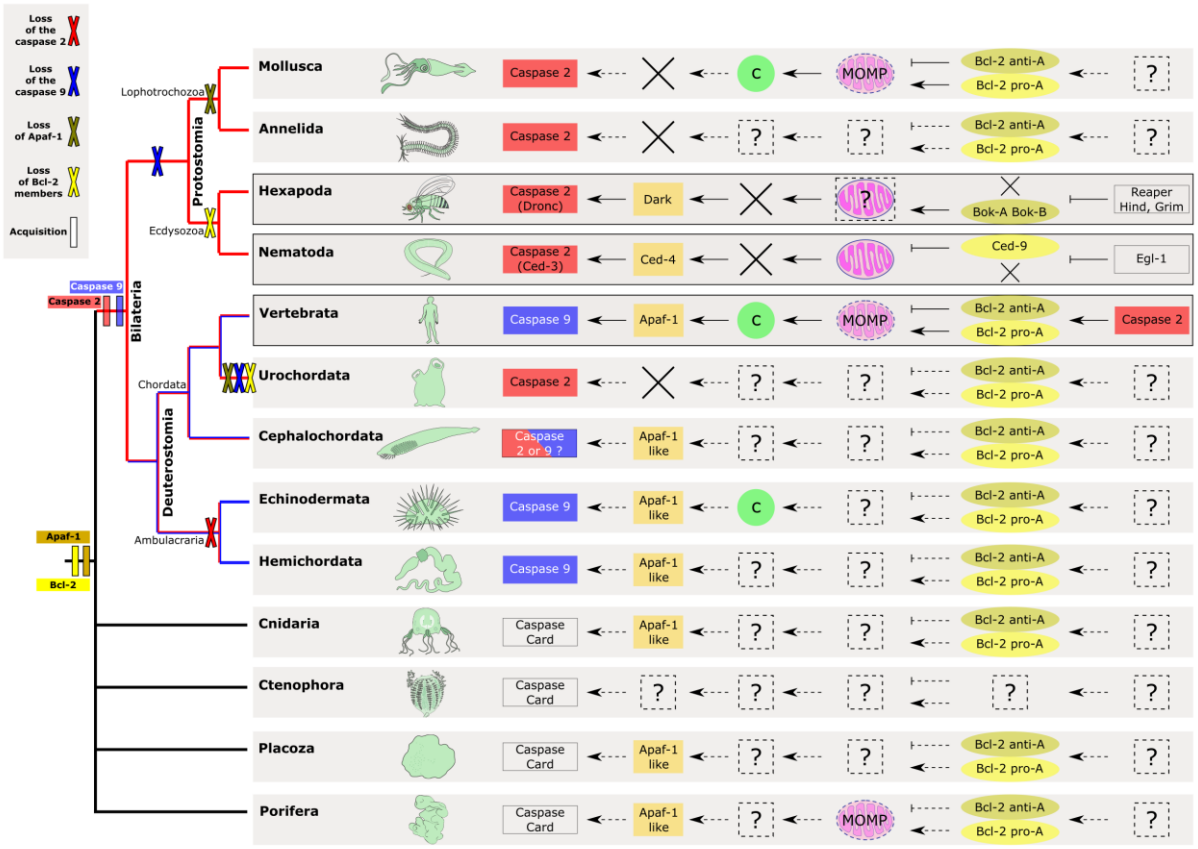

707

708 **Figure 2**

709 Reconstruction of convergent hypothetical intrinsic apoptotic pathways among metazoans
710 according to molecular actors detected and identified in their genomes. Variability of intrinsic
711 apoptotic pathways among animals emerged from convergences and recruitment of distinct

712 actors with independent evolutionary history. Caspase-2 is bilaterian-specific and the initiator
713 of ecdysozoans intrinsic apoptosis. Caspase-9 is restricted to deuterostomes and the specific
714 initiator of mammalian intrinsic apoptosis. Deuterostomes exhibit several losses (i.e. caspase
715 2 in cephalochordates, caspase 9 in urochordates) or duplication (i.e. caspase 9 in
716 echinoderms), highlighting a putative evolutionary flexibility in apoptotic pathway
717 establishment. Mitochondrial functions diverge among phyla and cytochrome c release thanks
718 to mitochondrial outer membrane permeabilisation (MOMP) is specific only to mammals and
719 possibly echinoderms. The convergent evolutionary histories reflect a probable phylum
720 specific adaptive process leading to parallel evolution of mitochondrial apoptotic pathways
721 observed among animals.
722
723
724
725
726
727

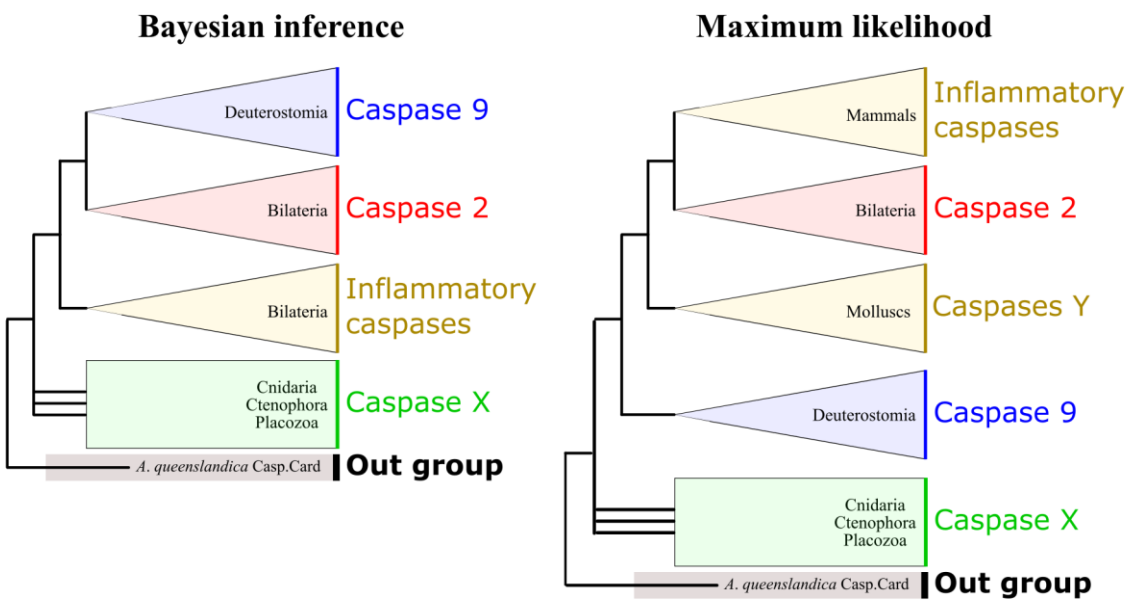

Supplementary Figure 1:

Monophyly of each CARD-caspase group is conserved using Bayesian inference and maximum likelihood analyses. Caspase-9, caspase-2 and [Inflammatory Caspases + Caspase-Y] groups remain conserved, confirming the bilaterian-specificity of caspase-2 and deuterostomian-specificity of caspase-9. Relationships among these three clades differ depending on the methodology employed. Divergent sequences of non-bilaterians animals (Cnidaria + Ctenophora + Placozoa) always form a paraphyletic group of caspases.

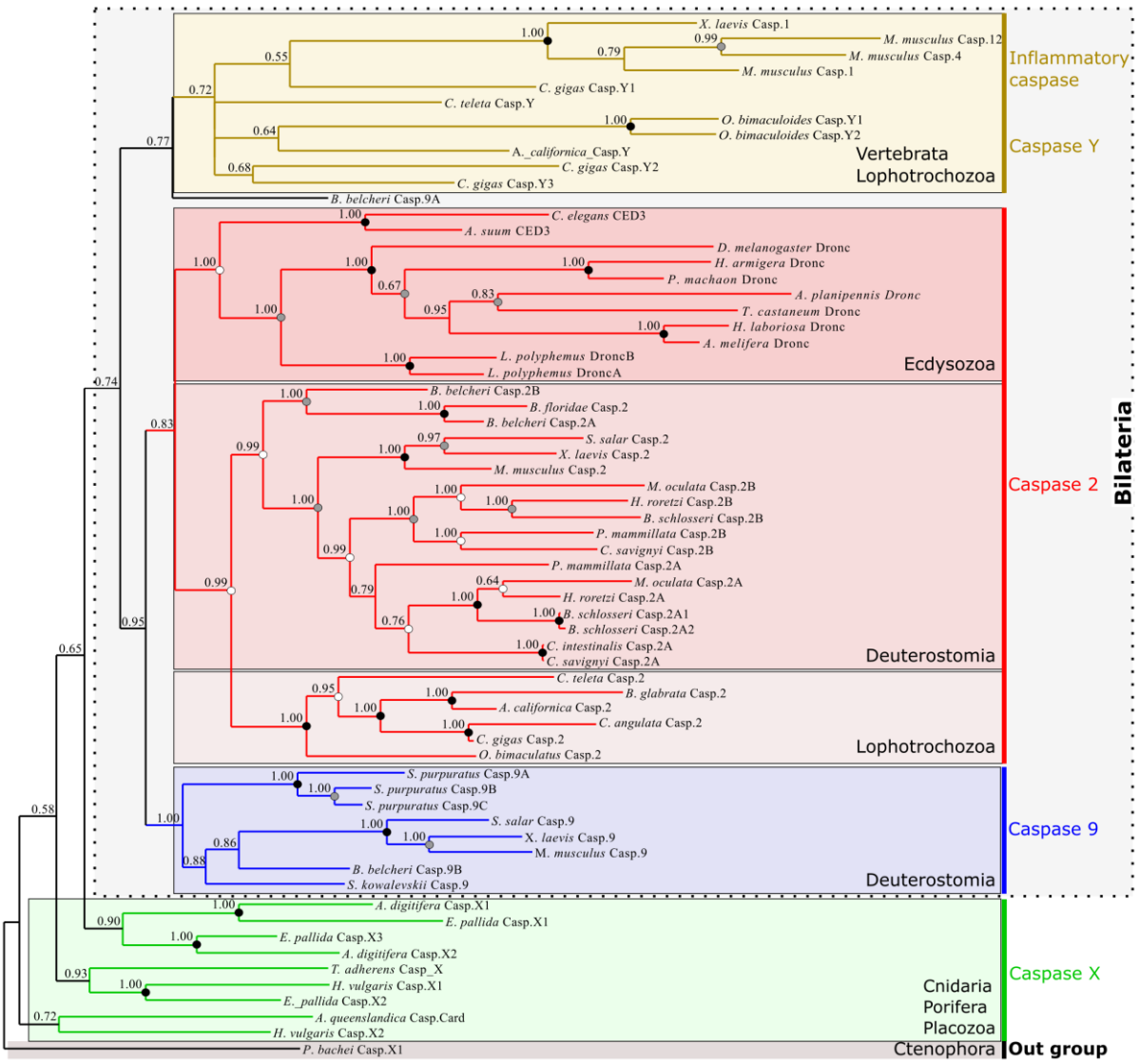

Supplementary Figure 2:

Topology of metazoan CARD-caspase phylogeny obtained by Bayesian inference. Selected outgroup is the unique CARD-caspase of Ctenophora *Pleurobrachia bachei.* The three strongly supported monophyletic groups identified, caspase-9, caspase-2 and [Inflammatory Caspases + Caspase-Y], are the same as when we used the unique CARD-caspase of the Porifera *Amphimedon queenslandica* as outgroup. Also, sequences from bilaterian animals remain monophyletic.

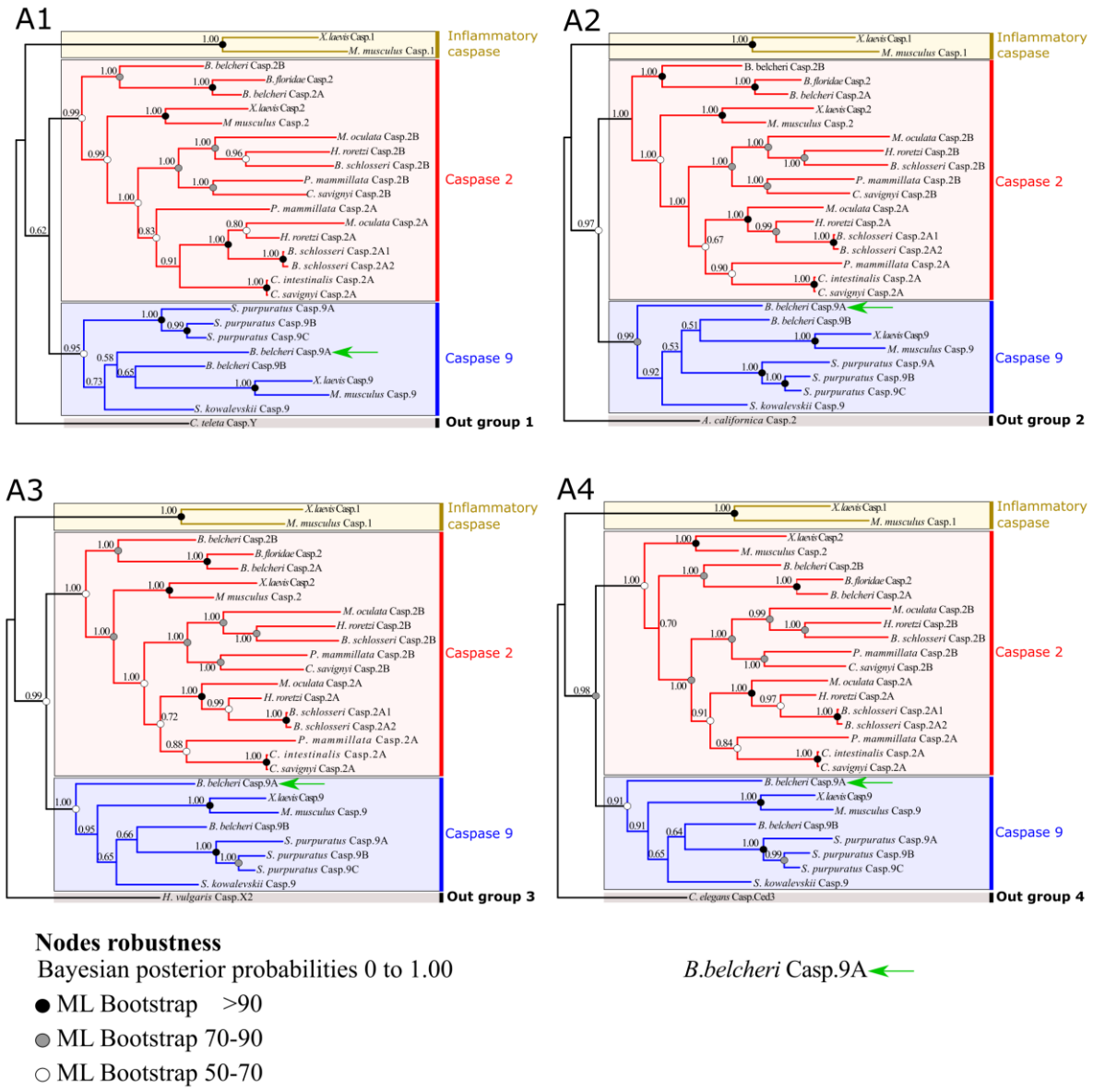

Supplementary Figure 3:

Phylogeny of CARD-caspases at the deuterostomian scale. Maximum likelihood and Bayesian inference methods produce similar topologies. Despite the unstable position of cephalochordate *Branchiostoma belcheri* caspase-9A (green arrow), it unequivocally appears to belong to the caspase-9 group. Numbers given correspond to posterior probabilities. We used respectively as outgroups *Capitella teleta* caspase-Y (ELT97848.1) (**A1**), *Aplysia*

760 *californica* caspase-2 (XP_005113266) (**A2**), *Hydra vulgaris* caspase-X2 (NP_001274285.1) (**A3**),

761 and *Caenorhabditis elegans* Ced3 (AAG42045.1) (**A4**).

762

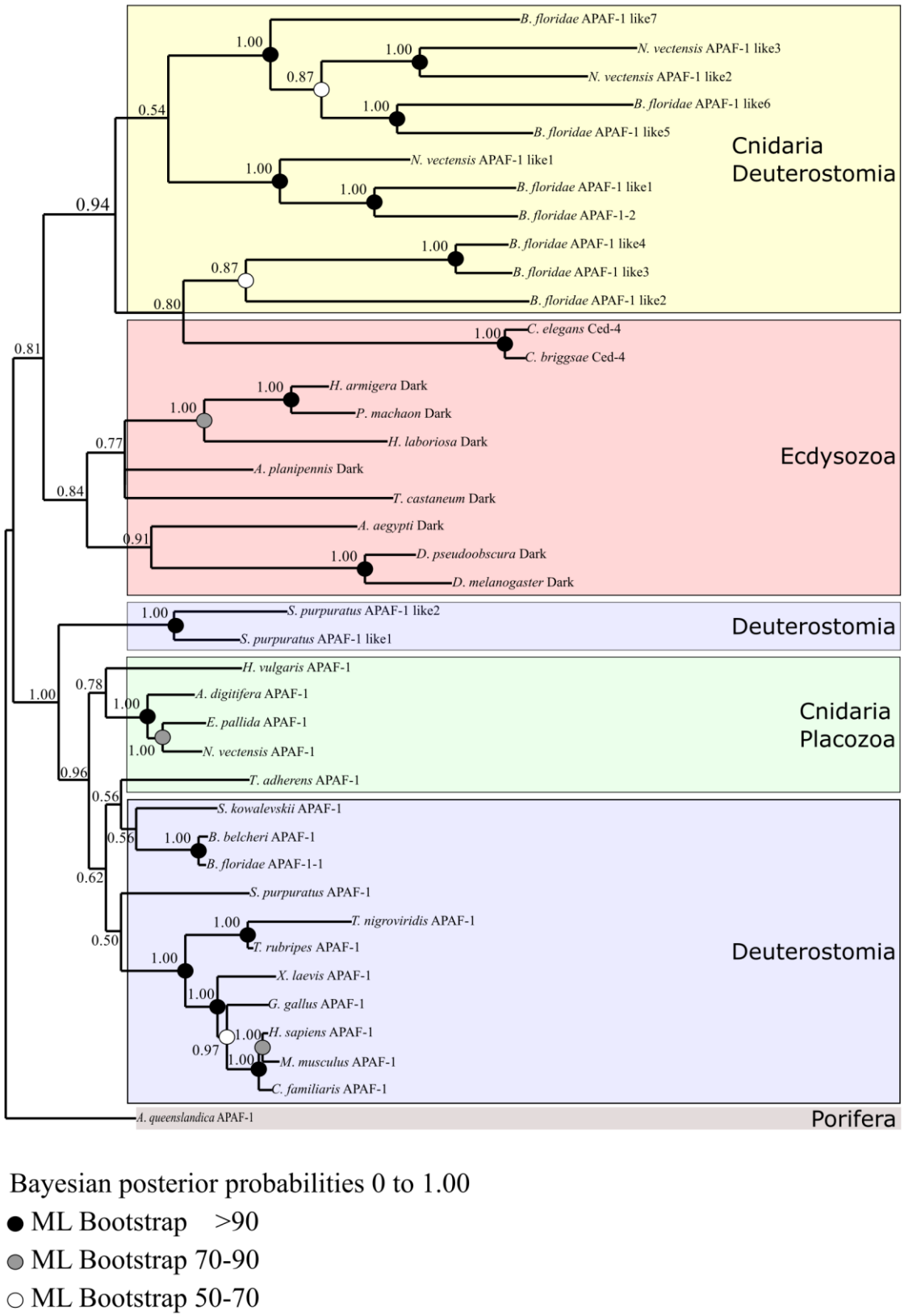

Supplementary Figure 4:

765 Phylogeny of Apaf-1 at the metazoan scale made with the NB-ARC domain alignment. Two
766 monophyletic groups are identified: Apaf-1 of ecdysozoans, and apaf-1 of [Deutostomia +
767 Cnidaria + Placozoa]. Globally, the topology is not consistent with the species phylogeny, and
768 nodes are poorly supported. Among metazoans, Apaf-1 is characterised by high sequence
769 divergence and fast independent evolution, making homology hypotheses difficult to establish.
770 The selected outgroup is Apaf-1 of Porifera *Amphimedon queenslandica*.
771
772
773
774
775
776
777
778
779
780
781
782
783
784
785
786
787
788

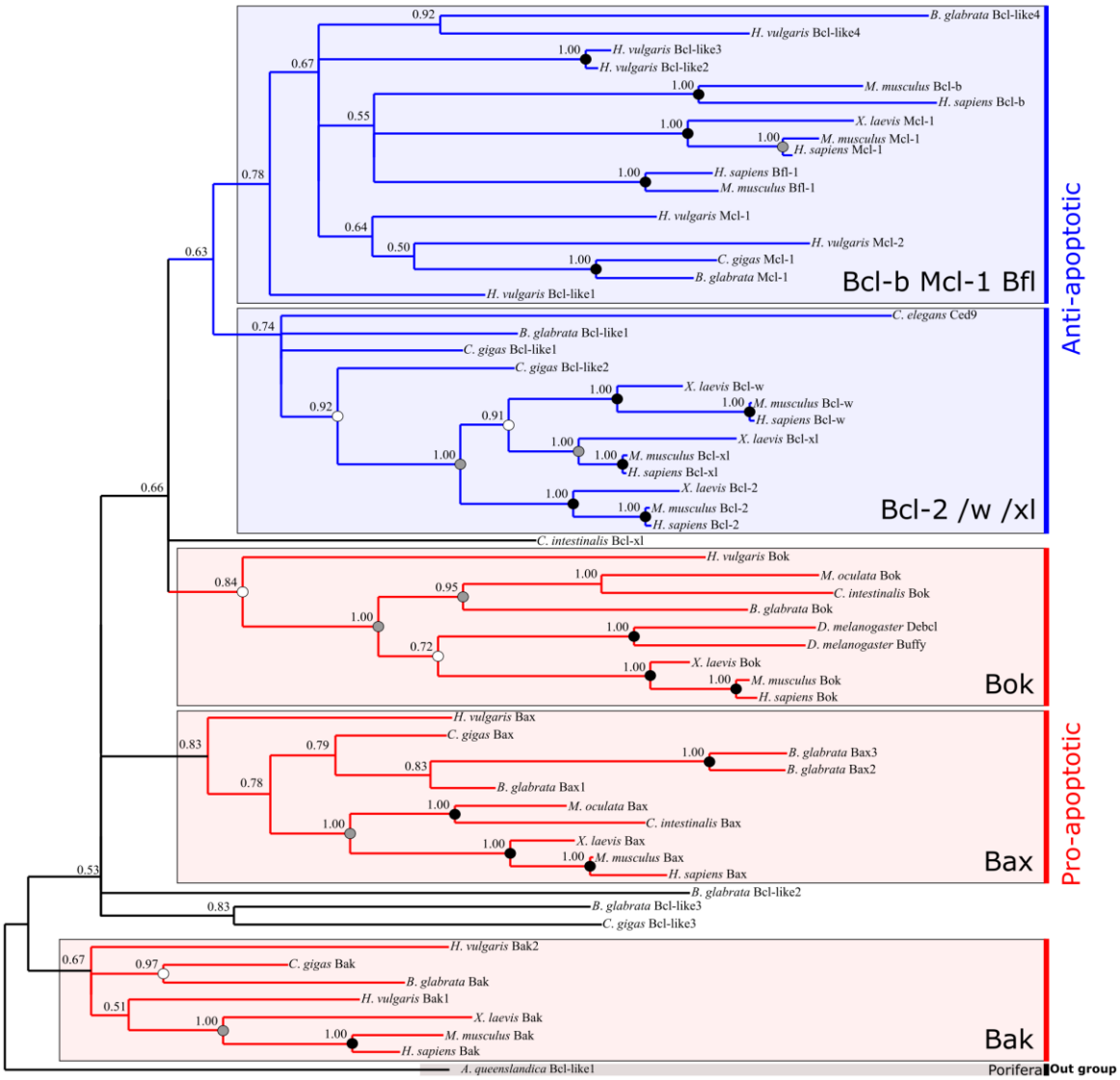

Bayesian posterior probabilities 0 to 1.00

● ML Bootstrap >90

● ML Bootstrap 70-90

○ ML Bootstrap 50-70

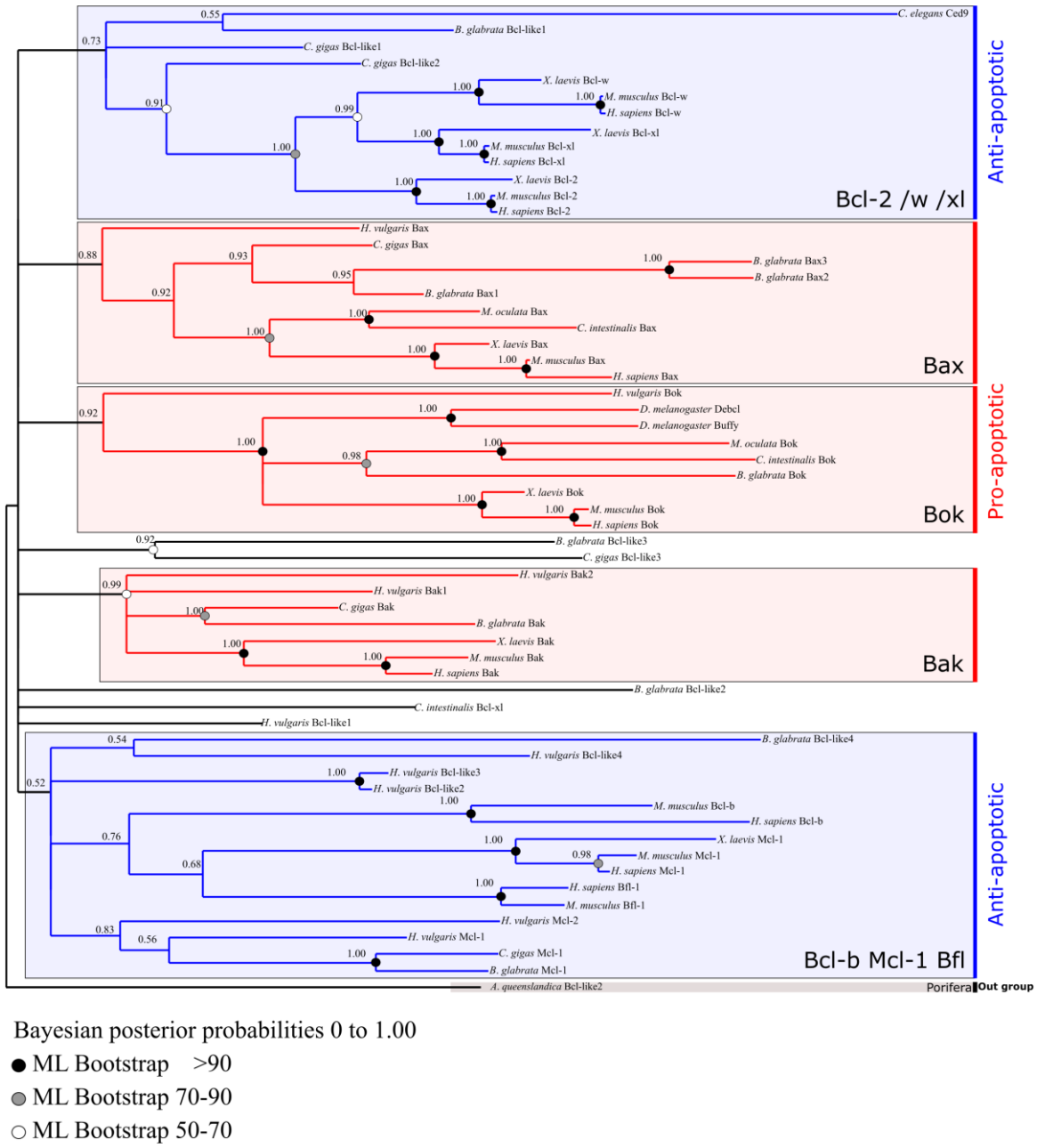

Supplementary Figure 5:

Topology of Bcl-2 family phylogeny from Bayesian inference and maximum likelihood at the metazoan scale using outgroups *Amphimedon queenslandica* Bcl-like 1 (XP_003383425.1) (**A**) and Bcl-like 2 (XP_003387574.1) (**B**). Bcl-2 proteins strictly clustered into five monophyletic groups: three 'pro-apoptotic' clades (Bok, Bak, Bax) and two less supported 'anti-apoptotic' groups (Bcl-2/W/XL) and a more complex (Bcl-B/Mcl-1/Bfl-1) clade. Each group includes bilaterian as well as non-bilaterian sequences which suggests a deep origin of this complex

804 multigenic family. Clustering into these five groups is consistent between analyses, while

805 relationships among them is not well resolved.

806
807
808
809
810
811
812
813
814
815
816
817
818
819
820
821
822
823 Supplemental table 1: List of CARD-caspases used for phylogenetic analysis.
824

Species		Accession number	Name
Porifera	*Amphimedon queenslandica*	XP_003383519.1	Casp. Card
Cnidaria	*Acropora digitifera*	XP_015766400.1	Casp. X2
		XP_015768208.1	Casp. X1
	Exaiptasia pallida	KXJ12672.1	Casp. X1
		KXJ20965.1	Casp. X2
		KXJ12683.1	Casp. X3
	Hydra vulgaris	ACY95435.1	Casp. X1
		ACY95436.1	Casp. X2
Ctenophora	*Pleurobrachia bachei*	Sb 2658116	Casp. X
Placozoa	*Trochoplax adherens*	RDD44781.1	Casp. X
Lophotrocozoa	*Aplysia californica*	XP_005113266.2	Casp. 2
		XP_012945422.1	Casp. Y
	Biomphalaria glabrata	XP_013082356.1	Casp. 2
	Capitella teleta	ELU00616.1	Casp. 2
		ELT97848.1	Casp. Y
	Crassostrea angulata	AGN75137.1	Casp. 2
	Crassostrea gigas	XP_011419292.2	Casp. 2
		XP_011414267.3	Casp. Y1
		XP_011449817.2	Casp. Y3
		XP_011432762.2	Casp. Y2
	Octopus bimaculoides	XP_014783442.1	Casp. 2
		XP_014790087.1	Casp. Y1
		XP_014784582.1	Casp. Y2
Chelicerata	*Limulus polyphemus*	XP_013788138.1	Casp. 2A

		XP_013776997.1	Casp. 2B
Insecta	*Agrilus planipennis*	XP_018324425.1	Casp. 2
	Apis melifera	XP_016771440.1	Casp. 2
	Drosophila melanogaster	CAB53565.1	Casp. 2
	Habropoda laboriosa	XP_017788772.1	Casp. 2
	Helicoverpa armigera	AEK20835.1	Casp. 2
	Papilio machaon	XP_014362236.1	Casp. 2
	Tribolium castaneum	XP_001813274.1	Casp. 2
Nematoda	*Ascaris suum*	ERG86894.1	Casp. 2
	Caenorhabditis elegans	AAG42045.1	Casp. 2
Vertebrata	*Salmo salar*	XP_014009539.1	Casp. 2
		XP_013991583.1	Casp. 9
	Mus musculus	NP_033937.2	Casp. 1
		EDL13489.1	Casp. 2
		NP_031635.2	Casp. 4
		AAH56447.1	Casp. 9
		AAT91067.1	Casp. 12
	Xenopus laevis	NP_001081223.1	Casp. 1
		NP_001081404.1	Casp. 2
		NP_001079035.1	Casp. 9
Echinodermata	*Strongylocentrotus purpuratus*	XP_789183.3	Casp. 9A
		XP_011661242.1 1	Casp. 9B
		XP_011661359.1	Casp. 9C
Hemichordata	*Saccoglossus kowalevskii*	XP_006811879.1	Casp. 9
Cephalochardata	*Branchiostoma belcheri*	XP_019646757.1	Casp. 2A
		XP_019642903.1	Casp. 2B
		XP_019623612.1	Casp. 9A
		XP_019644208.1	Casp. 9B
	Branchiostoma floridae	EEN68002.1	Casp. 2
Urochordata	*Botryllus schlosseri*	Boschl.CG.Botznik2013.chrUn.g02816.01.p	Casp. 2A1
		Boschl.CG.Botznik2013.chrUn.g08767.01.p	Casp. 2A2
		Boschl.CG.Botznik2013.chrUn.g09831.01.p	Casp. 2B
	Ciona intestinalis	KH2012:KH.C4.463.v1.A.ND1-1	Casp. 2A
	Ciona savignyi	CISAVI-CG-ENS81-R15-461426-463207-09349-P	Casp. 2A
		CISAVI-CG-ENS81-R54-461275-467018-10343-P	Casp. 2B
	Molgula oculata	Moocul-CG-ELv1_2-S113854-g13164-01-p	Casp. 2A
		Moocul-CG-ELv1_2-S103067-g09526-01-p	Casp. 2B
	Phallusia mammillata	PHMAMM-CG-MTP2014-S310-G07060-01-P	Casp. 2A
		PHMAMM-CG-MTP2014-S92-G02989-01-P	Casp. 2B
	Halocynthia roretzi	HARORE-CG-MTP2014-S35-G03390-01-P	Casp. 2A
		HARORE-CG-MTP2014-S130-G07320-01-P	Casp. 2B

Supplemental Table 2: Topology tests between Bayesian inference method (BI topology) and maximum likelihood estimation (ML topology). p-KH : p-value of one sided Kishino-Hasegawa

829 test. p-SH : p-value of Shimodaira-Hasegawa test. p-AU : p-value of approximately unbiased
830 (AU) test. In all cases, BI topology is more likelihood than the ML topology.
831

	p-KH	p-SH	p-AU
BI topology	0.714	1	0.702
ML topology	0.286	0.286	0.298

832
833
834
835
836 Supplemental Table 3: Estimation of the recombination (Rho) and substitution (Theta) rates
837 using ProteinEvolverABC on metazoans CARD-caspases alignment. The low rho values
838 indicate an absence of recombination and consequently no domain shuffling.
839

	Rho	Theta
Min.:	0.2762848	225.9003910
2.5% Perc.:	0.6311461	257.7492870
Median:	2.1534998	338.5860425
Mean:	2.0328712	332.1133675
Mode:	2.4251897	353.2953718
97.5% Perc.:	2.6993927	366.5018469
Max.:	2.7559795	367.8813704

840
841
842
843
844
845
846
847
848 Supplemental Table 4: List of Apaf-1 among metazoans. N/A: No APAF-1 has been identified.
849

Species		Accession number	Name
Porifera	*Amphimedon queenslandica*	XP_019855714.1	Apaf-1
Ctenophora	*Pleurobrachia bachei*	N/A	
Placozoa	*Trichoplax sp.*	RDD40813.1	Apaf-1
Cnidaria	*Acropora digitifera*	XP_015776356.1	Apaf-1
	Exaiptasia pallida	KXJ17575.1	Apaf-1
	Hydra vulgaris	CDG72123.1	Apaf-1
	Nematostella vectensis	XP_032220711.2	Apaf-1
		XP_032223290.2	Apaf-1 like1
		XP_001626725.1	Apaf-1 like2
		XP_032225984.2	Apaf-1 like3
Nematoda	*Caenorhabditis elegans*	CAA48781.1	Ced-4
	Caenorhabditis briggsae	XP_002642027.2	Ced-4
Insecta	*Aedes aegypti*	EAT48066.2	Dark
	Agrilus planipennis	XP_025834330.1	Dark
	Drosophila melanogaster	NP_725637.1	Dark

	Drosophila pseudoobscura	XP_001360832.3	Dark
	Habropoda laboriosa	XP_017794472.1	Dark
	Helicoverpa armigera	XP_021181657.1	Dark
	Papilio machaon	XP_014359375.1	Dark
	Tribolium castaneum	XP_015840766.1	Dark
Lophotrocozoa	*Aplysia californica*	N/A	
	Biomphalaria glabrata	N/A	
	Crassostrea angulata	N/A	
	Crassostrea gigas	N/A	
	Octopus bimaculoides	N/A	
	Capitella teleta	N/A	
Vertebrata	*Homo sapiens*	XP_047284715.1	Apaf-1
	Mus musculus	NP_033814.2	Apaf-1
	Canis lupus familiaris	XP_038544278.1	Apaf-1
	Gallus gallus	XP_040518239.1	Apaf-1
	Xenopus laevis	NP_001085834.1	Apaf-1
	Takifugu rubripes	XP_011611631.2	Apaf-1
	Tetraodon nigroviridis	CAG01878.1	Apaf-1
Echinodermata	*Strongylocentrotus purpuratus*	XP_030844937.1	Apaf-1
		XP_030854919.1	Apaf-1 like1
		XP_030828596.1	Apaf-1 like2
Hemichordata	*Saccoglossus kowalevskii*	XP_006818297.1	Apaf-1
Cephalochordata	*Branchiostoma belcheri*	XP_019621685.1	Apaf-1
	Branchiostoma floridae	XP_035681983.1	Apaf-1-1
		XP_035678916.1	Apaf-1-2
		XP_035672288.1	Apaf-1 like1
		XP_035690210.1	Apaf-1 like2
		XP_035667061.1	Apaf-1 like3
		XP_035696241.1	Apaf-1 like4
		XP_035693308.1	Apaf-1 like5
		XP_035673101.1	Apaf-1 like6
		XP_035692718.1	Apaf-1 like7
Urochordata	*Botryllus schlosseri*	N/A	
	Ciona intestinalis	N/A	
	Ciona savignyi	N/A	
	Molgula oculata	N/A	
	Phallusia mammillata	N/A	
	Halocynthia roretzi	N/A	

Supplemental table 5: List of Bcl-2 used for phylogenetic analysis.

856

Species		Accession number	Names
Porifera	*Amphimedon queenslandica*	XP_003383425.1	Bcl-2 like 1
		XP_003387574.1	Bcl-2 like 2
Cnidaria	*Hydra vulgaris*	EF104645.1	Bak 1
		EU035760.1	Bak 2
		XP_012562061.1	Bax
		EU035764.1	Bcl-2 like 1
		EF104646.1	Bcl-2 like 2
		EU035765.1	Bcl-2 like 3
		EU035763.1	Bcl-2 like 4
		EU035761.1	Bok
		EF104647.1	Mcl-1 1
		EU035762	Mcl-1 2
Nematoda	*Caenorhabditis elegans*	AAA20080.1	Ced-9
Insecta	*Drosophila melanogaster*	AAF44120.1	Buffy (Bok-1)
		AAF26289.1	Buffy (Bok-2)
Lophotrocozoa	*Biomphalaria glabrata*	XP_013085524.1	Bax 1
		XP_013096338_1	Bax 2
		XP_013086802.1	Bax 3
		XP_013070177.1	Bak
		XP_013081872.1	Bcl-2 like 1
		XP_013093137.1	Bcl-2 like 2
		XP_013068612.1	Bcl-2 like 3
		XP_013083436.1	Bcl-2 like 4
		XP_013069706.1	Bok
		XP_013065969.1	Mcl-1
	Crassostrea gigas	XP_011424481.1	Bax
		XP_011439700.1	Bak
		XP_011449013.1	Bcl-2 like 1
		ACH42081.1	Bcl-2 like 2
		EKC18663.1	Bcl-2 like 3
		XP_011436990.1	Mcl-1 1
		EKC40007.1	Mcl-1 2
Vertebrata	*Homo sapiens*	AAA74466.1	Bak
		NP_001278357.1	Bax
		API71171.1	Bcl-2
		AAK48715.1	Bcl-B
		AAB09055.1	Bcl-w
		CAA80661.1	Bcl-xL
		NP_004040.1	Bfl-1
		NP_115904.1	Bok
		AAF64255.1	Mcl-1
	Mus musculus	NP_031549.2	Bak
		NP_031553.1	Bax
		AAH95964.1	Bcl-2
		Q9Z0F3.1	Bcl-B

		AAA51039.1	Bcl-xL
		AAB09056.1	Bcl-w
		Q07440.1	Bfl-1
		NP_058058.1	Bok
		NP_032588.1	Mcl-1
	Xenopus laevis	NP_001089587.1	Bak
		AAR84081.1	Bax
		BAH28834.1	Bcl-2
		AAI10791.1	Bcl-xl
		XP_018089640.1	Bcl-w
		NP_001139563.1	Bok
		ACI47310.1	Mcl-1
Urochordata	*Ciona intestinalis*	KH2012:KH.C4.794.v1.A.SL1-1	Bax
		KH2012:KH.S653.2.v2.A.SL1-1	Bcl-xl
		KH2012:KH.L87.39.v1.A.ND1-1	Bok
	Molgula oculata	Moocul.CG.ELv1_2.S96550.g08147.01.p	Bax
		Moocul.CG.ELv1_2.S112899.g12639.01.p	Bok